JOURNAL OF AGRICULTURAL AND FOOD CHEMISTRY

Article

pubs.acs.org/JAFC

Effects of pH on the Molecular Binding between β-Lactoglobulin and Bixin

Yue Zhang,[†] Edward Wright,[‡] and Qixin Zhong*[,†]

[†]Department of Food Science and Technology and [‡]Department of Biochemistry and Cellular and Molecular Biology, University of Tennessee, Knoxville, Tennessee 37996, United States

ABSTRACT: Binding between β-lactoglobulin (β-Lg), the major whey protein, and bixin, the major carotenoid in annatto, was studied at pH 3.0−10.0. The Fourier transform infrared spectroscopy and UV−vis absorption spectroscopy results showed that the binding involved a complex formation. The tryptophan quenching fluorescence and analytical ultracentrifugation data showed that there were two specific binding sites and that the binding affinity increased significantly with an increase in pH. A higher efficiency of energy transfer from tryptophan fluorescence to bixin was observed at higher pH. Thermodynamic parameters and the number of specific binding sites obtained from isothermal titration calorimetry and analytical ultracentrifugation suggested that binding involved mostly hydrophobic interactions for the two specific binding sites. The impacts of pH on binding were correlated to the conformation of β-Lg, the hydrophobic pocket of which becomes more available at higher pH and ionic strength.

KEYWORDS: *bixin−β-lactoglobulin binding, pH, spectroscopy, isothermal titration calorimetry, analytical ultracentrifugation, circular dichroism*

INTRODUCTION

β-Lactoglobulin (β-Lg), the most abundant whey protein in dairy products, is a small globular extracellular protein. One major characteristic of β-Lg is its ability to bind various hydrophobic ligands into its β-barrel calyx.[1] Due to its availability and diverse functional properties, β-Lg has been studied extensively for various applications, including encapsulation of carotenoids such as curcumin.[2] In contrast to advances in applications, fundamental understanding of molecular interactions between hydrophobic food components and β-Lg is scarce. It is well established that the structure of β-Lg, including conformation and the monomer−dimer equilibrium, has been studied for variables such as pH, temperature, and ionic strength.[1,3] These variables in turn are expected to affect ligand−protein binding, which, however, is an understudied research area.

In this work, molecular binding between bixin and β-Lg was studied at different pH conditions using complementary techniques of Fourier transform infrared (FTIR) spectroscopy, UV−vis absorption spectroscopy, fluorescence spectroscopy, analytical ultracentrifugation (AUC), isothermal titration calorimetry (ITC), and circular dichroism (CD). Bixin was chosen as a model carotenoid because it is the major coloring component of annatto, which is used as a pigment in many food products. Bixin is an unusual carotenoid with a free carboxyl end group and another esterified carboxyl end group (Scheme 1).[4] Comprehensive understanding of bixin−β-Lg binding may also shed light on the biological fate of other carotenoids, especially those that play an important role in human health as anti-inflammatory agents, antioxidants, and anticancer agents.[5,6]

Scheme 1. Molecular Structure of Bixin

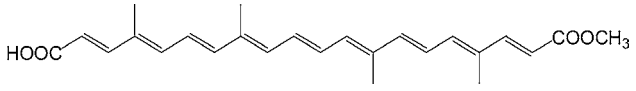

MATERIALS AND METHODS

Materials. β-Lg was purchased from Sigma-Aldrich Corp. (St. Louis, MO, USA). Bixin was obtained from Faltz-Bauer, Inc. (Waterbury, CT, USA). Other chemicals were procured from either Sigma-Aldrich or Fisher Scientific (Pittsburgh, PA, USA). Protein solution was prepared in a 0.01 M phosphate buffer (PBS) adjusted to different pH values using either 1 N HCl or 1 N NaOH and kept in the dark at 4 °C before use. Bixin was dissolved in ethanol at a concentration of 0.1 M as a stock solution that was diluted with PBS to 5 mM before use.

Fourier Transform Infrared (FTIR) Spectroscopy. The FTIR instrument was a Nicolet Nexus 670 FT-IR spectrometer (Thermo Nicolet Corp., Madison, WI, USA) equipped with a germanium attenuated total reflection (ATR) accessory, a DTGS KBr detector, and a KBr beam splitter. All spectra were taken via the ATR method with a resolution of 4 cm^{-1} using 64 scans. β-Lg was prepared in deuterated water to prevent the interference of hydrogen bonds in the amide region of the protein spectra.[7] For the same reason, bixin was dissolved in DMSO because the amount of DMSO in β-Lg solution has no absorbance in the 1850−1500 cm^{-1} range of the IR spectrum.[8]

UV−Vis Absorption Spectroscopy. The concentration of β-Lg was prepared at 1.0×10^{-5} M. The UV−vis absorption spectra were acquired between 200 and 800 nm using a UV−vis spectrometer (Unicam, Cambridge, UK). All experiments were performed in triplicate at room temperature (21 °C).

Fluorescence Spectroscopy. The fluorescence spectra were recorded using an RF-1501 spectrofluorometer (Shimadzu Corp., Tokyo, Japan). The excitation wavelength was 285 nm, and the

Received: September 5, 2012
Revised: December 6, 2012
Accepted: January 7, 2013
Published: January 8, 2013

emission spectra were recorded between 300 and 450 nm. Both the excitation and emission slit widths were set at 10 nm. The background fluorescence was calibrated using PBS. Samples were measured in triplicate.

The fluorescence quenching data can be analyzed using the well-known Stern−Volmer equation:

$$\frac{F_0}{F} = 1 + k_q\tau_0[Q] = 1 + K_{SV}[Q] \quad (1)$$

where F_0 and F are the fluorescence intensities in the absence and presence of a quencher, [Q] is the concentration of the quencher, K_{SV} is the Stern−Volmer quenching constant, k_q is the biomolecular quenching constant, and τ_0 is the lifetime of fluorescence in the absence of a quencher and equals 10^{-8} s.[9]

Fluorescence quenching can be classified as dynamic quenching, static quenching, or both. Static quenching refers to the formation of a complex between the fluorophore and quencher, whereas dynamic quenching refers to the collisional encounters between the fluorophore and quencher. When static quenching and dynamic quenching both occur for the same quencher, the Stern−Volmer plot does not exhibit a straight line but an upward (concave) curvature at high [Q], and the relationship between F_0/F and [Q] can be described by the following modified form of the Stern−Volmer equation:[10]

$$\frac{F_0}{F} = (1 + K_D[Q])(1 + K_S[Q]) \quad (2)$$

K_D and K_S are dynamic and static quenching constants, respectively.

Analysis of Energy Transfer between β-Lg and Bixin Using Förster's Nonradiative Energy Transfer (FRET) Theory. Using the FRET theory, the distance r between the donor and the acceptor can be calculated by the equation[9]

$$E = 1 - \frac{F}{F_0} = \frac{R_0^6}{R_0^6 + r^6} \quad (3)$$

where E is the efficiency of energy transfer between the donor and acceptor and R_0 is the critical distance when the efficiency of transfer is 50%, estimated by

$$R_0^6 = 8.79 \times 10^{-25} K^2 N^{-4} \phi J \quad (4)$$

where K^2 is the orientation factor of a dipole and is 2/3 for the random orientation as in a solution, N is the refractive index of the medium, ϕ is the fluorescence quantum yield of the donor, and J is the overlap integral of the fluorescence emission spectrum of the donor and the absorption spectrum of the receptor, which can be calculated by eq 5:

$$J = \frac{\int_0^\infty F(\lambda)\varepsilon(\lambda)\lambda^4 \, d\lambda}{\int_0^\infty F(\lambda) \, d\lambda} \quad (5)$$

$F(\lambda)$ is the corrected fluorescence intensity of the donor at wavelength λ and $\varepsilon(\lambda)$ is the molar absorption coefficient of the acceptor at wavelength λ.

Analytical Ultracentrifugation (AUC). AUC analyses were performed at 298 K on a Beckman XL-I analytical ultracentrifuge (Beckman Coulter, Inc., Palo Alto, CA, USA) equipped with an An50Ti rotor. Absorbance at 280 nm for protein and 346 nm for bixin and interference scans were recorded every 5 min. Samples contained 0.05 mM β-Lg and 0, 0.1, 0.25, or 0.5 mM bixin and were adjusted to pH 4.0, 7.4, and 9.0 using 1 N HCl or NaOH. The molecular weight (M) and the sedimentation coefficient distribution, $c(s)$, were determined by analysis using SEDFIT. The equilibrium dissociation constant (K_D) for bixin and β-Lg was determined by fitting the data to a two-site mass balance conservation model using GraphPad Prism 6.0 software (San Diego, CA, USA).

Isothermal Titration Calorimetry (ITC). A Microcal VP-ITC microcalorimeter (Microcal, Northampton, MA, USA) was used in this set of experiments conducted at 293 K. Bixin prepared at 5 mM in 5% ethanol was used as a titrant. The protein solutions were also prepared in PBS buffers containing 5% ethanol. Solutions were degassed prior to each titration, where 1.451 mL of a protein solution was loaded in the sample cell and was mixed with 4 μL of the titrant in each injection. During injection of the titrant, the injection syringe was programmed at 307 rpm to enable rapid mixing but without foaming. The thermal effect due to mixing and dilution was calibrated by a control experiment, where the titrant was injected into the PBS without protein. Sedphat (v.8.01) was used for ITC data analysis using a nonsymmetrical two-site model. Error ranges were determined by critical chi-squared reduction at the 68% confidence level for each parameter.

Circular Dichroism (CD). A model 202 CD spectrometer (Aviv Biomedical, Inc., Lakewood, NJ, USA) was used to collect far-UV CD spectra between 200 and 260 nm at 298 K, with an interval of 1 nm. The 0.05 mM β-Lg was contained in a quartz cell with a 0.1 cm path length, and a constant nitrogen flush was used throughout the experiments. With the SELCON 3 method available in the CDPro software, the CD spectra were used to determine secondary structure contents of β-LG by referencing to 43 soluble proteins with known precise secondary structures.[11] Triplicate samples were measured.

RESULTS AND DISCUSSION

FTIR Spectra of β-Lg before and after Interaction with Bixin. FT-IR spectroscopy is a valuable method to monitor the changes in the secondary structure of proteins and their dynamics when interacting with other compounds. In the IR region, the bands corresponding to the amide I (80% C═O stretch, 1600−1700 cm^{-1}), II (60% N—H bend and 40% C—N stretch, near 1550 cm^{-1}), and III (40% C—N stretch, 30% N—H bend, near 1300 cm^{-1}) vibrations are generally employed to study protein structure.[12] Curve a in Figure 1 shows the FT-IR spectrum of β-Lg in D_2O. Due to the substitution of N−H by N−D, the shape of the amide II band and the wavenumber corresponding to the band center (1534 cm^{-1}) are different from the measurement from aqueous solutions.[13,14] Curve b shows the spectrum of β-Lg after the addition of bixin. The peak position shifted from 1646 to 1639 cm^{-1} for amide I and from 1534 to 1551 cm^{-1} for amide II after interaction with bixin. The FTIR spectra changes indicate a complex formation between β-Lg and bixin and changes in the secondary structure of β-Lg.[7]

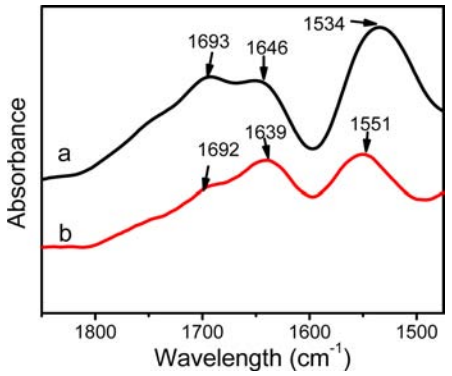

Figure 1. FT-IR spectra of β-Lg in the absence (curve a) and presence (curve b) of bixin. The concentrations of β-Lg and bixin are both 0.5 mM.

UV−Vis and Fluorescence Spectra of β-Lg under Different pH Conditions. The UV−vis absorption spectra of β-Lg showed a UV absorption band centered on about 280 nm (Figure 2), reflecting the presence of residues such as tryptophan (Trp) and tyrosine (Tyr). The absorption bands around 280 nm were stronger at a higher pH, implying that the

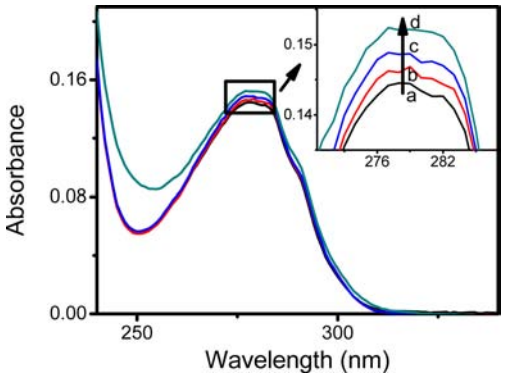

Figure 2. UV absorption spectra of β-Lg at different pH conditions. Curves a, b, c, and d correspond to pH 3.0, 5.6, 7.4, and 10.0, respectively.

structure of β-Lg was altered when the pH was changed from acidic to alkaline conditions.

Because β-Lg has two Trp residues (Trp-19 and Trp-61) that possess intrinsic fluorescence, the effect of pH on protein structure can be revealed by fluorescence spectra. Figure 3

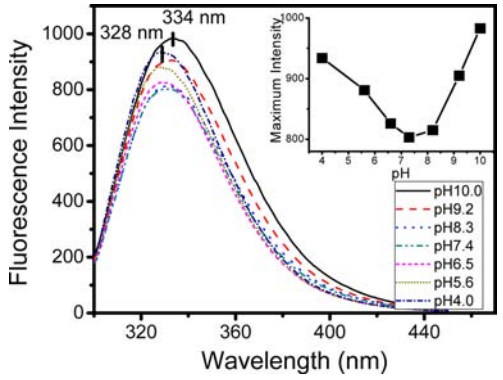

Figure 3. Fluorescence spectra of β-Lg at different pH conditions, with the maximum intensity presented in the inset. The excitation wavelength was 285 nm, and the concentration of β-Lg was 0.01 mM.

shows that the fluorescence intensity decreased when the pH increased from 4.0 to 7.4 and then rose to the maximum at pH 10. This illustrated that the tertiary structure of the protein was altered when the pH was changed from acidic to neutral and from neutral to basic conditions. In addition, the center of the emission peak shifted from 328 to 334 nm when the pH increased from 4.0 to 10.0. The red shift of the emission maximum indicates the increased solvent polarity around the Trp residues and the decreased protein hydrophobicity, which reflects conformational changes of β-Lg.

Fluorescence Quenching Studies of β-Lg–Bixin Binding under Different pH Conditions. The emission spectra of β-Lg showed that the fluorescence intensity of β-Lg decreased significantly with the increase of bixin concentration, demonstrated in Figure 4 for data at pH 7.4. Plots of the Stern–Volmer equation at pH 3.0–10.0 in Figure 5A show upward curvatures at high bixin concentrations, indicating that both static and dynamic quenchings were involved in binding. However, for lower bixin concentrations (C_{bixin}/ $C_{\beta\text{-Lg}} < 5$), the Stern–Volmer curves are linear (Figure 5B), and the data can be analyzed using eq 1, with constants listed in Table 1. The

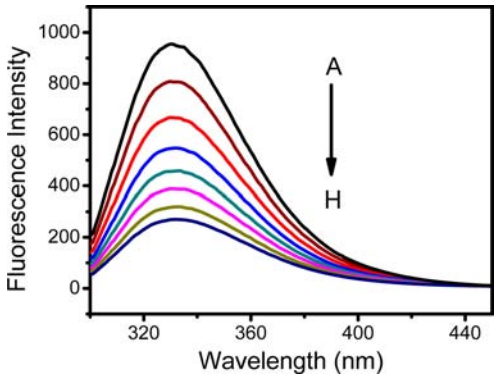

Figure 4. Effect of bixin on the fluorescence spectra of β-Lg at 298 K and pH 7.4. The concentration of β-Lg was 1.0×10^{-5} M, and the concentrations of bixin were 0, 1, 2, 3, 4, 5, 6, and 7×10^{-5} M, corresponding to curves A–H.

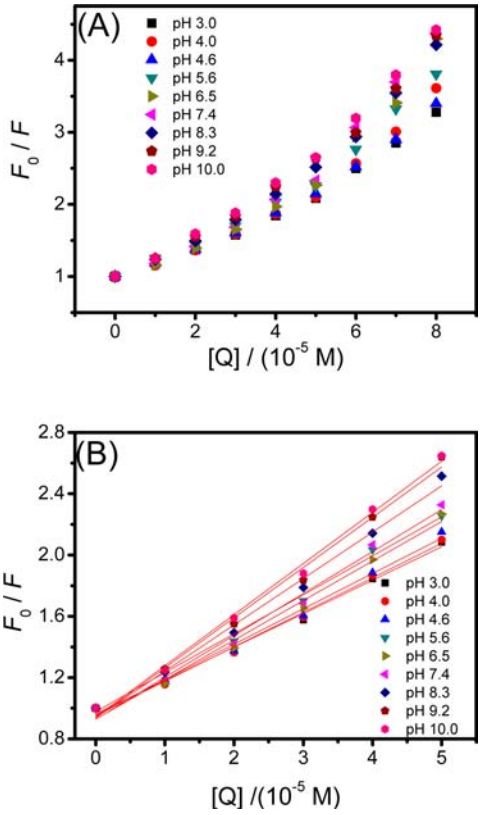

Figure 5. Plots of F_0/F for β-Lg against [Q] for the entire bixin range of 0–0.08 mM (A) and the lower concentration range of 0–0.05 mM (B) under different pH conditions. The concentration of β-Lg was 1.0×10^{-5} M.

bigger Stern–Volmer constant indicates stronger binding between bixin and β-Lg at a higher pH in the range of 3.0–10.0.

A linear Stern–Volmer plot represents a single quenching mechanism, either static or dynamic. For dynamic quenching, the maximum collisional quenching constant of various quenchers is 2.0×10^{10} M^{-1} s^{-1}.[15] The k_q in this work (Table 1) is 2 orders of magnitude larger than 2.0×10^{10} M^{-1} s^{-1}, suggesting that the quenching process between bixin and β-Lg is mainly due to static quenching by complex formation.[9] Therefore, the K_{SV} obtained according to eq 1 can be treated as a static quenching constant.[16] The analysis is further supported

dx.doi.org/10.1021/jf303844w | J. Agric. Food Chem. 2013, 61, 947–954

Table 1. Quenching Constants K_{SV} and k_q and the Number of Binding Sites (n) Derived from Stern−Volmer Plots Due to Binding between Bixin and β-Lg at Different pH Conditions and 298 K

pH	K_{SV} ($\times 10^4$ M^{-1})	k_q ($\times 10^{12}$ M^{-1} s^{-1})	R^s	SD^b	n
3.0	2.18	2.18	0.992	0.009	1.1
4.0	2.24	2.24	0.991	0.009	1.2
4.6	2.31	2.31	0.990	0.010	1.1
5.6	2.54	2.54	0.993	0.010	1.0
6.5	2.58	2.58	0.986	0.014	1.3
7.4	2.73	2.73	0.985	0.015	1.2
8.3	3.02	3.02	0.989	0.014	1.2
9.2	3.28	3.28	0.988	0.016	1.2
10.0	3.33	3.33	0.994	0.012	1.2

[s]Correlation coefficient from linear regression of Stern−Volmer plots. [b]Standard deviation from linear regression of Stern−Volmer plots.

by changes in the FTIR spectrum of protein (Figure 1), which is not characteristic of the collision (dynamic quenching).

For static quenching, in the linear range of the above Stern−Volumer curve, the number of binding sites (n) can be obtained according to eq 6 when small molecules independently bind to a set of equivalent sites on a macromolecule.[17] The number of binding sites estimated on the basis of eq 6 is approximately 1 and is similar at all pH conditions (Table 1).

$$\log \frac{F_0 - F}{F} = \log K_b + n \log[Q] \quad (6)$$

Effect of Ionic Strength on the Binding between Bixin and β-Lg. To study the impact of ionic strength, an additional set of K_{SV} was estimated at 0.5 M NaCl (Table 2). Contrasting

Table 2. Effect of pH on the Stern−Volmer Quenching Constant of Bixin Binding to β-Lg in the Presence of 0.5 M NaCl at 298 K

pH	K_{SV} ($\times 10^4$ M^{-1})	R	SD
3.0	3.33	0.985	0.009
4.0	3.27	0.987	0.010
5.6	3.17	0.980	0.018
6.5	3.03	0.993	0.007
7.4	3.00	0.989	0.009
8.3	3.11	0.991	0.008
9.2	3.60	0.996	0.003
10.0	3.84	0.984	0.010

a monotonic increase of K_{SV} with an increase in pH at 0 mM NaCl (Table 1), the K_{SV} at 0.5 M NaCl first decreased and then increased as the pH increased from pH 3.0 to 10.0, with a minimum of 3.0×10^4 M^{-1} at pH 7.4. Because a higher ionic strength weakens electrostatic interactions and strengthens surface hydrophobicity of proteins, the larger binding constant at a higher ionic strength suggests the importance of hydrophobic interaction in the formation of bixin−β-Lg complexes.[18]

Energy Transfer between β-Lg and Bixin. The FRET theory is a nondestructive spectroscopy method that can be used to determine the mean distance between amino acid residues (the donor) and bound molecules (the acceptor). According to this theory, the distance r, the critical distance R_0, and the efficiency of energy transfer E between bixin and β-Lg can be calculated by eqs 3−5.

Using data at pH 7.4 for an example, the fluorescence and absorption spectra at equal molarity of β-Lg and bixin are plotted in Figure 6, and the J value was determined to be 6.88×10^{-15} cm^3 M^{-1}. Using an N value of 1.4, a ϕ value of 0.12,[15] and 2/3 for K^2, R_0 was calculated to be 3.53 nm on the basis of eq 4. The experimental value of F/F_0 gave an E value of 0.164, which in turn enabled the determination of binding distance (r) to be 4.63 nm. The estimated r values are listed in Table 3 and are in

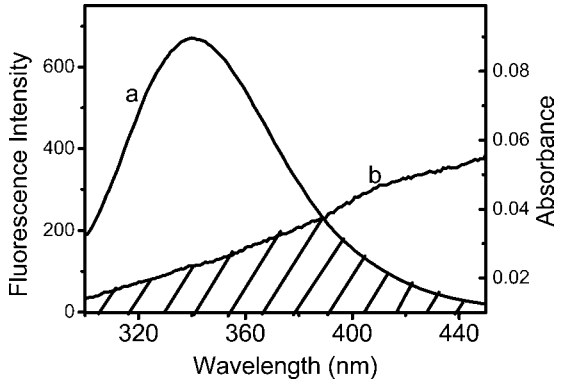

Figure 6. Overlap of β-Lg fluorescence (a) and bixin absorption (b) spectra at pH 7.4 and 298 K at equal β-Lg and bixin concentrations of 1.0×10^{-5} M.

Table 3. Energy Transfer Parameters for Bixin−β-Lg Interactions As Affected by pH at 298 K

pH	r (nm)	R_0 (nm)	E	$10^{15}J$ (cm^3 L mol^{-1})
3.0	4.99	3.32	0.080	4.761
4.0	4.98	3.40	0.092	5.446
4.6	4.73	3.43	0.127	5.827
5.6	4.82	3.48	0.124	6.289
6.5	4.72	3.49	0.140	6.388
7.4	4.63	3.53	0.164	6.876
8.3	4.54	3.56	0.188	7.296
9.2	4.27	3.63	0.274	8.123
10.0	4.11	3.65	0.329	8.463

the range between 2 and 8 nm expected for a donor fluorophore and acceptor fluorophore.[19] Furthermore, because β-Lg contains two Trp residues, both have to be taken into account when the efficiency of energy transfer is calculated. The r values are between $0.5R_0$ and $1.5R_0$ (Table 3), suggesting they are the average values of bixin binding to two Trp residues of β-Lg and a high possibility of energy transfer from β-Lg to bixin. The R_0 estimated in our work is similar to the 3.4 nm calculated for retinol binding with β-Lg,[20,21] suggesting the likelihood of bixin binding with β-Lg through the same binding site located in the β-barrel of the protein.[20,21] In addition, Fugate et al.[22] suggested that large R_0 values indicate proximity of the ligand only to one Trp residue. With the assumption that the efficient fluorescence energy transfer from β-Lg to bixin is mainly by one Trp, the calculated energy transfer parameters from β-Lg to bixin at different pH conditions are presented in Table 3. The larger E value and the smaller r value at higher pH indicate higher energy transfer efficiency, which agrees with the larger values of K_{SV} at higher pH (Table 1).

AUC Analysis of Binding between Bixin and β-Lg. AUC was used to further investigate the binding affinity between β-Lg and bixin at pH 4.0, 7.4, and 9.0. The

sedimentation profiles of β-Lg were similar at pH 7.4 and 9.0 (Figure 7A), corresponding to M of 17.6 kDa and indicating

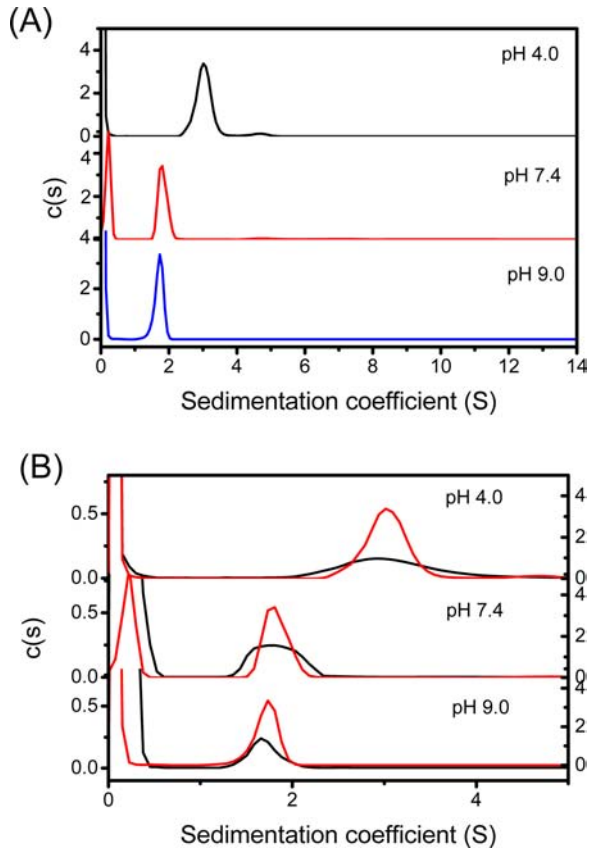

Figure 7. Analytical ultracentrifugation analysis of a mixture with 50 μM β-Lg and 250 μM bixin adjusted to pH 4.0, 7.4, and 9.0: (A) interference data showing the position of β-Lg monomer and dimer; (B) data collected at 346 nm (for bixin, black) and 280 nm (for β-Lg) in the same experiment.

the predominantly monomeric form of the protein. At pH 4.0, a major early fraction of sediments at 3.5 S and two later fractions at 8.6 and 12.5 S were observed. The major fraction corresponded to M of 37.1 kDa, that is, the dimeric form of β-Lg. The later fractions were estimated to have M of 166 and 290 kDa, which agrees with the reported few oligomers of β-Lg at pH 4.0.[3]

To determine the amount of bixin bound to β-Lg, AUC experiments were performed at three bixin concentrations at each pH condition. Figure 7B shows the treatment with 50 μM β-Lg and 250 μM bixin at three pH conditions. The sedimentation profile shows free bixin at ~0.2 S and bixin−β-Lg complex at ~2 S. By fitting the data using the two-site model, the amount of bound bixin and the dissociation constant (K_D) to each site were determined (Table 4). The data showed that β-Lg has a primary and a secondary binding site. A larger amount of bixin bound with β-Lg at higher pH, agreeing with a lower K_D, which indicates higher binding affinity. A comparison of K_D for the two binding sites additionally showed that pH had a greater impact on the secondary binding site (bigger variation of K_D for site II, Table 4). Furthermore, the $1/K_D$ for site I from AUC (Table 4) has a magnitude similar to K_{SV} estimated from fluorescence data (Table 1), suggesting the fluorescence is mainly contributed by the primary binding site.

Table 4. Binding of Different Amounts of Bixin to 50 μM β-Lg Determined by Mass Analysis of AUC Data

			K_D[a] (μM)	
pH	total bixin (μM)	bound bixin (μM)	site I	site II
4.0	100	16 ± 3	180 ± 40	2100 ± 430
	250	28 ± 4		
	500	42 ± 4		
7.4	100	30 ± 4	110 ± 26	880 ± 140
	250	54 ± 6		
	500	81 ± 7		
9.0	100	36 ± 5	98 ± 21	640 ± 90
	250	65 ± 7		
	500	86 ± 8		

[a]Dissociation constant obtained by fitting the data to the two-site model in Prism 6.0.

Calorimetric Characterization of Binding between Bixin and β-Lg at Different pH Conditions. ITC has become a common method to characterize biomolecular binding. The technique enables the determination of thermodynamic parameters such as enthalpy change (ΔH), entropy change (ΔS), binding stoichiometry (m), and binding constant (K_a) in one experiment.[23] Figure 8 shows representative calorimetric profiles and the calculated energy changes during the titration of bixin into β-Lg at 293 K. The thermodynamic parameters obtained by using the non-symmetric two-site model are presented in Table 5. In agreement with the fluorescence and AUC results, the lower K_D with increasing pH indicates an increase in binding affinity. A marginally favorable enthalpy was observed at each pH with a more favorable ΔH at the secondary site relative to the primary binding site in each case. The entropic contribution was also favorable at both sites at each pH. At site I, the entropy becomes more favorable at higher pH. Thus, the increase in affinity at the primary site as pH increases is driven by increasing ΔS. The role of entropy in the binding process is consistent with hydrophobic interactions contributing significantly to the bixin−β-LG binding.[24]

Conformation Changes of β-Lg upon Interacting with Bixin at Different pH Conditions. The far-UV CD spectra were acquired to study secondary structure changes of β-Lg before and after interaction with bixin at different pH conditions, shown in Figure 9 for one acidic (pH 4.0) and one alkaline (pH 8.5) condition. In the absence of bixin, a wide valley around 216 nm characteristic of a β-sheet dominant protein[25] was observed at both pH conditions. The different intensity minima around 216 nm suggest that the structure of β-Lg is different at these two pH conditions. The valley shifted to a higher wavelength around 220 nm after titration by bixin, and the valley minimum became less negative. Changes in CD spectra suggest the binding by bixin changed secondary structures of β-Lg. Specific secondary structure changes at different pH conditions are summarized in Table 6. An increased content of β-sheet structure was observed after binding with bixin at acidic conditions, but the opposite was observed at pH above 7.4. In contrast, the content of α-helical structure increased at all pH conditions (between 3.0 and 10.0) after binding with bixin.

Impacts of pH and Ionic Strength on Binding As Interpreted by β-Lg Structure. Because the overall

dx.doi.org/10.1021/jf303844w | J. Agric. Food Chem. 2013, 61, 947−954

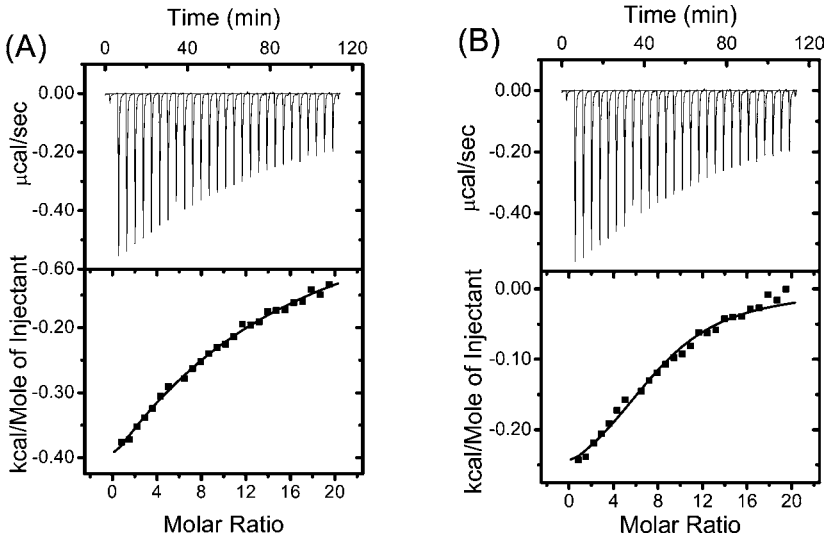

Figure 8. Titration profiles at 293 K when a titrant of 5 mM bixin was mixed at 4 μL per injection with a solution containing 50 μM β-Lg at pH 4.0 (A) and 9.0 (B).

Table 5. Thermodynamic Properties for Binding between Bixin and β-Lg at Different pH Values at 293 K

pH		K_D (μM)	ΔG (kcal mol^{-1})	ΔH (kcal mol^{-1})	$-T\Delta S$ (kcal mol^{-1})
4.0	site I	250 ± 36	−4.8	−2.1 ± 0.3	−2.7
	site II	1400 ± 210	−3.8	−2.9 ± 0.4	−0.9
7.4	site I	130 ± 19	−5.2	−1.2 ± 0.1	−4.0
	site II	810 ± 120	−4.1	−2.0 ± 0.3	−2.1
9.0	site I	79 ± 11	−5.5	−1.0 ± 0.1	−4.5
	site II	340 ± 51	−4.7	−3.1 ± 0.2	−1.6

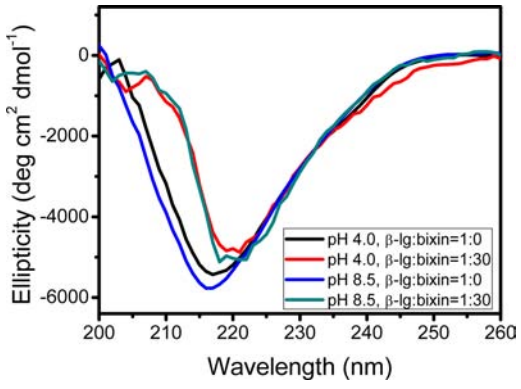

Figure 9. Circular dichroism spectra of β-Lg before and after mixing with bixin at a protein/bixin molar ratio of 1:30 at pH 4.0 and 8.5. The test temperature was 298 K.

Table 6. Secondary Structures of β-Lg As Affected by Complexation with Bixin under Different pH Conditions (T = 298 K)

pH	molar ratio of β-Lg/bixin	α-helix (%)	β-sheet (%)	turn (%)	unordered (%)
3.0	1:0	9.0	32.3	22.9	36.3
	1:30	9.5	32.5	21.0	37.5
4.0	1:0	7.3	34.5	22.9	35.9
	1:30	10.3	35.7	23.0	31.8
5.0	1:0	6.5	33.8	23.0	36.3
	1:30	7.0	35.2	21.6	38.5
6.4	1:0	7.2	34.0	22.8	36.5
	1:30	11.5	34.3	21.4	33.5
7.4	1:0	7.8	32.6	23.8	36.9
	1:30	7.6	29.6	20.9	38.8
8.5	1:0	8.1	31.2	24.0	36.8
	1:30	9.8	29.0	20.3	36.9
10.0	1:0	5.9	32.8	23.0	39.2
	1:30	7.1	31.4	20.1	39.3

equilibrium in the system, that is, the influence of protein structure and solvent, is taken into account in the protein−ligand binding process, the present study does not represent an accurate binding location and thermodynamic interpretation for bixin on β-Lg but provides the "apparent location" to explain the microscopic environment around the bixin−β-Lg complex. The impacts of pH and ionic strength on K_{SV} and $1/K_D$ are quite in agreement with β-Lg structures suggested in the literature. β-Lg contains a β-barrel (calyx) formed by eight antiparallel β-stands, labeled A−H in Figure 10, that form flexible and mobile loops, with loops AB, CD, EF, and GH more mobile than other loops.[26] The β-barrel is known as a pocket providing the primary binding site for nonpolar molecules. The space between the outer surface of the β-barrel and an adjacent α-helix is believed to be a secondary specific

dx.doi.org/10.1021/jf303844w | J. Agric. Food Chem. 2013, 61, 947−954

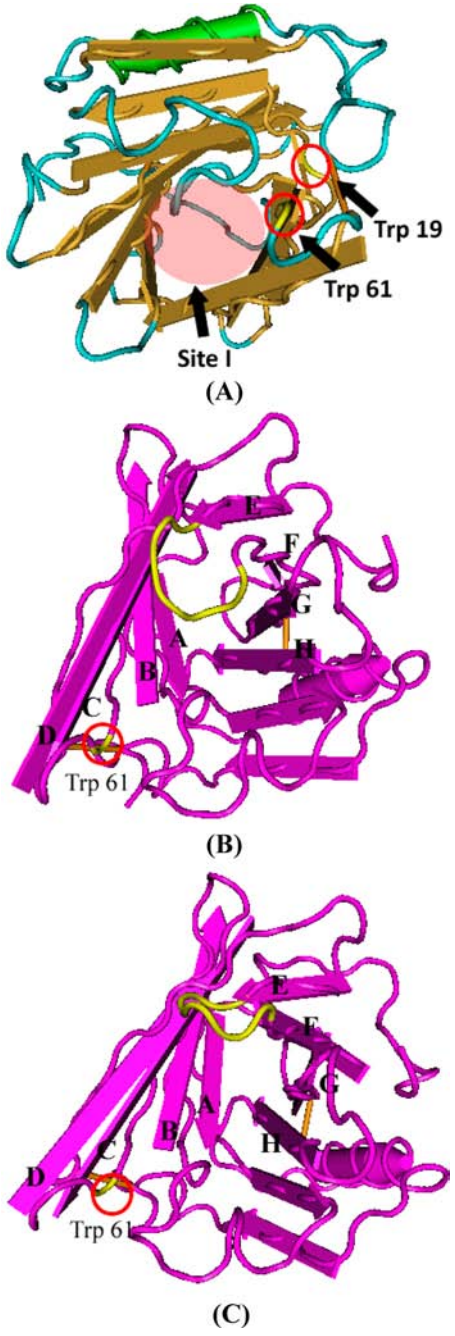

Figure 10. Crystal structures of β-Lg as affected by pH. (A) Tertiary structure of β-Lg at physiologic pH. The protein backbone is shown by tube worm (blue), helix (the substantial arrow, green), and strand (the compressed arrow, golden), and the two Trp residues (Trp-19 and Trp-61) are shown in yellow. (B) Tertiary structure of β-Lg at acidic pH. (C) Tertiary structure of β-Lg at alkaline pH. The EF loop is shown in yellow. The images were generated from the Cn3D program (NCBI) using the structure of Qin et al.[28].

binding site (Figure 10A).[27] The EF loop acts as a flap over the primary binding site.[28] Because Trp-61 is within the mobile CD loop (Figure 10A) of the calyx, whereas Trp-19 is a little far away from the primary binding site, the fluorescence data in this work can be considered to have a major contribution from Trp-61.[26]

The impacts of pH on β-Lg structure have been well studied, described as the Tanford transition.[28,29] At low pH and low ionic strength (Figure 10B), the EF loop is closed, and the binding is inhibited. The transition is triggered by the protonation of Glu-89, causing the opening of EF-loop flap at higher pH and enabling the hydrophobic cavity of the β-barrel available for binding with compounds in the continuous phase. At low ionic strength, the monotonic increase of K_{SV} with an increase in pH (Table 1) is in agreement with the position of EF loop as affected by pH. At higher ionic strength, the EF loop opens to a greater extent and the binding with hydrophobic bixin is enhanced, consistent with higher values of K_{SV} (Table 2 versus Table 1). In addition, Wu et al.[30] reported that palmitic acid binds to the binding site of β-Lg through not only hydrophobic interactions but also electrostatic interactions resulting from the carboxylate headgroup of the fatty acid. In our case, bixin also has a carboxylate headgroup, and electrostatic forces may also have contributed to the binding with basic amino acid residues such as lysine, tyrosine, and arginine that have pK_a values of 10.6, 10, and 12.0, respectively.[31] The binding between cationic amino acid residues and anionic bixin is expected to be weaker at higher pH because of the higher extent of deprotonation, which is opposite from the current findings for specific bindings. Therefore, hydrophobic interactions are the major force contributing to the binding between bixin and β-Lg at sites I and II. Finally, the β-barrel structure remains unchanged at pH 7.0−10.0,[32,33] and the β-barrel structure integrity on binding between β-Lg and bixin is not expected to be a factor at the conditions studied in the present work.

In summary, findings from this study suggest that β-Lg and bixin form complexes mainly driven by hydrophobic interactions. Under the studied experimental conditions, the hydrophobic pocket of β-Lg is the primary binding site. The fluorescence quenching data revealed that binding is favored at higher pH and higher ionic strength, which promotes the opening of the hydrophobic pocket. Binding parameters obtained from AUC and ITC data suggested the presence of a secondary specific binding site that is also favored at higher pH.

AUTHOR INFORMATION

Corresponding Author

*Postal address: Department of Food Science and Technology, The University of Tennessee, 23 Food Safety and Processing Building, 2605 River Drive, Knoxville, TN 37996, USA. Phone: (865) 974-6196. Fax: (865) 974-7332. E-mail: qzhong1@utk.edu.

Funding

We are grateful for the financial support from The University of Tennessee and the Dairy Research Institute (Rosemont, IL, USA).

Notes

The authors declare no competing financial interest.

REFERENCES

(1) Sakurai, K.; Konuma, T.; Yagi, M.; Goto, Y. Structural dynamics and folding of β-lactoglobulin probed by heteronuclear NMR. *Biochim. Biophys. Acta−Gen. Subj.* **2009**, *1790*, 527−537.

(2) Sneharani, A. H.; Karakkat, J. V.; Singh, S. A.; Rao, A. G. A. Interaction of curcumin with β-lactoglobulin-stability, spectroscopic analysis, and molecular modeling of the complex. *J. Agric. Food Chem.* **2010**, *58*, 11130−11139.

(3) Gottschalk, M.; Nilsson, H.; Roos, H.; Halle, B. Protein self-association in solution: the bovine β-lactoglobulin dimer and octamer. *Protein Sci.* **2003**, *12*, 2404−2411.
(4) Bouvier, F.; Dogbo, O.; Camara, B. Biosynthesis of the food and cosmetic plant pigment bixin (annatto). *Science* **2003**, *300*, 2089−2091.
(5) Zsila, F.; Molnar, P.; Deli, J.; Lockwood, S. F. Circular dichroism and absorption spectroscopic data reveal binding of the natural *cis*-carotenoid bixin to human α(1)-acid glycoprotein. *Bioorg. Chem.* **2005**, *33*, 298−309.
(6) Kandansamy, K.; Somasundaram, P. D. Microencapsulation of colors by spray drying − a review. *Int. J. Food Eng.* **2012**, 8.
(7) Qi, Z. D.; Zhou, B.; Xiao, Q.; Shi, C.; Liu, Y.; Dai, J. Interaction of rofecoxib with human serum albumin: determination of binding constants and the binding site by spectroscopic methods. *J. Photochem. Photobiol. A−Chem.* **2008**, *193*, 81−88.
(8) Zhou, B.; Qi, Z. D.; Xiao, Q.; Dong, J. X.; Zhang, Y. Z.; Liu, Y. Interaction of loratadine with serum albumins studied by fluorescence quenching method. *J. Biochem. Biophys. Methods* **2007**, *70*, 743−747.
(9) Lakowicz, J. R. *Principles of Fluorescence Spectroscopy*, 2nd ed.; Plenum Press: New York, 1999.
(10) Vaughn, W. M.; Weber, G. Oxygen quenching of pyrenebutyric acd fluorescence in water. A dynamic probe of microenvironment. *Biochemistry* **1970**, *9*, 464−473.
(11) Whitmore, L.; Wallace, B. A. DICHROWEB, an online server for protein secondary structure analyses from circular dichroism spectroscopic data. *Nucleic Acids Res.* **2004**, *32*, W668−W673.
(12) Pelton, J. T.; McLean, L. R. Spectroscopic methods for analysis of protein secondary structure. *Anal. Biochem.* **2000**, *277*, 167−176.
(13) Kandori, H.; Maeda, A. FTIR spectroscopy reveals microscopic structural-changes of the protein around the rhodopsin chromophore upon photoisomerization. *Biochemistry* **1995**, *34*, 14220−14229.
(14) Bhattacharjee, C.; Saha, S.; Biswas, A.; Kundu, M.; Ghosh, L.; Das, K. P. Structural changes of β-lactoglobulin during thermal unfolding and refolding − an FT-IR and circular dichroism study. *Protein J.* **2005**, *24*, 27−35.
(15) Lange, D. C.; Kothari, R.; Patel, R. C.; Patel, S. C. Retinol and retinoic acid bind to a surface cleft in bovine β-lactoglobulin: a method of binding site determination using fluorescence resonance energy transfer. *Biophys. Chem.* **1998**, *74*, 45−51.
(16) Gauthier, T. D.; Shane, E. C.; Guerin, W. F.; Seitz, W. R.; Grant, C. L. Fluorescence quenching method for determining equilibrium-constants for polycyclic apromatic-hydrocarbons binding to dissolved humic materials. *Environ. Sci. Technol.* **1986**, *20*, 1162−1166.
(17) Kang, J.; Liu, Y.; Xie, M. X.; Li, S.; Jiang, M.; Wang, Y. D. Interactions of human serum albumin with chlorogenic acid and ferulic acid. *Biochim. Biophys. Acta−Gen. Subj.* **2004**, *1674*, 205−214.
(18) Kato, A.; Matsuda, T.; Matsudomi, N.; Kobayashi, K. Determination of protein hydrophobicity using a sodium dodecyl-sulfate binding method. *J. Agric. Food Chem.* **1984**, *32*, 284−288.
(19) Weiss, S. Fluorescence spectroscopy of single biomolecules. *Science* **1999**, *283*, 1676−1683.
(20) Chakraborty, J.; Das, N.; Halder, U. C. Unfolding diminishes fluorescence resonance energy transfer (FRET) of lysine modified β-lactoglobulin: relevance towards anti-HIV binding. *J. Photochem. Photobiol. B−Biol.* **2011**, *102*, 1−10.
(21) Andrade, S. M.; Costa, S. M. B. Spectroscopic studies on the interaction of a water soluble porphyrin and two drug carrier proteins. *Biophys. J.* **2002**, *82*, 1607−1619.
(22) Fugate, R. D.; Song, P. S. Spectroscopic characterization of β-lactoglobulin−retinol complex. *Biochim. Biophys. Acta* **1980**, *625*, 28−42.
(23) Frazier, R. A.; Papadopoulou, A.; Green, R. J. Isothermal titration calorimetry study of epicatechin binding to serum albumin. *J. Pharm. Biomed. Anal.* **2006**, *41*, 1602−1605.
(24) Hattori, T.; Hallberg, R.; Dubin, P. L. Roles of electrostatic interaction and polymer structure in the binding of β-lactoglobulin to anionic polyelectrolytes: Mmeasurement of binding constants by frontal analysis continuous capillary electrophoresis. *Langmuir* **2000**, *16*, 9738−9743.
(25) Xiuqi, Z.; Keiderling, T. A. Lipid-induced conformational transitions of β-lactoglobulin. *Biochemistry* **2006**, *45*, 8444−8452.
(26) Kontopidis, G.; Holt, C.; Sawyer, L. The ligand-binding site of bovine β-lactoglobulin: evidence for a function? *J. Mol. Biol.* **2002**, *318*, 1043−1055.
(27) Hasni, I.; Bourassa, P.; Tajmir-Riahi, H. A. Binding of cationic lipids to milk β-lactoglobulin. *J. Phys. Chem. B* **2011**, *115*, 6683−6690.
(28) Qin, B. Y.; Bewley, M. C.; Creamer, L. K.; Baker, H. M.; Baker, E. N.; Jameson, G. B. Structural basis of the tanford transition of bovine β-lactoglobulin. *Biochemistry* **1998**, *37*, 14014−14023.
(29) Sakurai, K.; Goto, Y. Dynamics and mechanism of the Tanford transition of bovine β-lactoglobulin studied using heteronuclear NMR spectroscopy. *J. Mol. Biol.* **2006**, *356*, 483−496.
(30) Wu, S. Y.; Perez, M. D.; Puyol, P.; Sawyer, L. β-Lactoglobulin binds palmitate within its central cavity. *J. Biol. Chem.* **1999**, *274*, 170−174.
(31) Walstra, P. *Physical Chemistry of Foods*; CRC Press: Boca Raton, FL, 2003.
(32) Mercadé-Prieto, R.; Paterson, W. R.; Wilson, D. I. The pH threshold in the dissolution of β-lactoglobulin gels and aggregates in alkali. *Biomacromolecules* **2007**, *8*, 1162−1170.
(33) Taulier, N.; Chalikian, T. V. Characterization of pH-induced transitions of β-lactoglobulin: ultrasonic, densimetric, and spectroscopic studies. *J. Mol. Biol.* **2001**, *314*, 873−889.